AGU PUBLICATIONS

Geophysical Research Letters

RESEARCH LETTER
10.1002/2015GL063555

Key Points:
- Diel changes in O_2/Ar were used to determine mixed layer ecosystem metabolism
- Estimated metabolic rates agreed well with other independent methods
- There was a net production of O_2 in the mixed layer during the sampling period

Supporting Information:
- Figure S1
- Figure S2
- Figures S1 and S2 captions and Table S1

Correspondence to:
S. Ferrón,
sferron@hawaii.edu

Citation:
Ferrón, S., S. T. Wilson, S. Martínez-García, P. D. Quay, and D. M. Karl (2015), Metabolic balance in the mixed layer of the oligotrophic North Pacific Ocean from diel changes in O_2/Ar saturation ratios, *Geophys. Res. Lett.*, *42*, 3421–3430, doi:10.1002/2015GL063555.

Received 19 FEB 2015
Accepted 7 APR 2015
Accepted article online 14 APR 2015
Published online 5 MAY 2015

©2015. American Geophysical Union. All Rights Reserved.

Metabolic balance in the mixed layer of the oligotrophic North Pacific Ocean from diel changes in O_2/Ar saturation ratios

Sara Ferrón[1,2], Samuel T. Wilson[1,2], Sandra Martínez-García[1,2,3], Paul D. Quay[4], and David M. Karl[1,2]

[1]Daniel K. Inouye Center for Microbial Oceanography: Research and Education, University of Hawai'i at Mānoa, Honolulu, Hawaii, USA, [2]Department of Oceanography, School of Ocean and Earth Science and Technology, University of Hawai'i at Mānoa, Honolulu, Hawaii, USA, [3]Now at Centre for Ecology and Evolution in Microbial Model Systems, Linnaeus University, Kalmar, Sweden, [4]School of Oceanography, University of Washington, Seattle, Washington, USA

Abstract In situ measurements were made to determine oxygen (O_2) metabolic balance in the upper oligotrophic ocean from diel changes in O_2 to argon (Ar) ratios. The study took place during 13–24 March 2014, at the Hawaii Ocean Time-series Station ALOHA (A Long-term Oligotrophic Habitat Assessment), in the North Pacific Subtropical Gyre. Microbial community respiration and gross O_2 production, estimated from in situ diel changes in O_2/Ar saturation, agreed well with those calculated using other independent methods. Net oxygen production (NOP), estimated from in situ diel changes in O_2/Ar saturation, showed large day-to-day variability. However, when averaged over the entire observational period, mean diel NOP was in relatively good agreement with the estimated mean steady state NOP (9.2 ± 9.3 mmol O_2 m^{-2} d^{-1} compared to 11.7 ± 1.1 mmol O_2 m^{-2} d^{-1}, respectively).

1. Introduction

Net community production (NCP) of organic matter in the upper ocean is an important term in the oceanic carbon (C) cycle as it sets an upper limit on organic C export to the deep ocean and, in turn, the amount of carbon dioxide (CO_2) that the oceans can remove from the atmosphere. We still do not fully understand the processes controlling NCP or how it may be affected by climate-driven changes in sea surface temperature and stratification. The subtropical oligotrophic gyres occupy ~40% of the Earth's surface [*Karl and Church*, 2014], and therefore, quantifying NCP in these vast ecosystems is critical for our understanding of the oceanic C cycle. However, the low biological activity associated with subtropical oligotrophic gyres makes quantification of rates of gross primary production (GPP) and microbial community respiration (MCR) in these sites a challenge. The balance between GPP and MCR, i.e., NCP, is at least an order of magnitude smaller, and hence, even more difficult to measure. The clear disagreement between NCP estimates inferred from in vitro and in situ measurements in the euphotic layer of the oligotrophic ocean [*Williams et al.,* 2013] has led to a still unresolved debate about whether these large areas of the ocean are net heterotrophic or net autotrophic [*del Giorgio et al.,* 1997; *Duarte et al.,* 2013; *Ducklow and Doney*, 2013; *Karl et al.,* 2003; *Williams*, 1998; *Williams et al.,* 2013]. *Williams et al.* [2013] concluded that in vitro O_2 measurements cause a bias in NCP toward net heterotrophy and questioned whether these biases applied to other incubations-based methods, such as ^{14}C-bicarbonate fixation. In addition to the potential containment effects of incubation experiments, in vitro and in situ methods often represent different time scales, with the former resolving short-term variability (~12–24 h) and the latter normally representing a time-integrated value (~1–2 weeks), which further complicates direct comparison. For example, it has been suggested that geochemical in situ methods incorporate infrequent productivity bursts that are often missed in short-time incubations [*Karl et al.,* 2003].

The O_2/Ar method has proven to be a valuable tool to estimate NCP in the upper ocean from individual measurements, when gas exchange, entrainment, and advection can be constrained or measured [e.g., *Hamme and Emerson*, 2006; *Kaiser et al.,* 2005; *Quay et al.,* 2010; *Reuer et al.,* 2007]. This method is commonly based on the assumption of steady state conditions and cannot capture short-term variability in NCP. Recently, *Hamme et al.* [2012] and *Tortell et al.* [2014] independently reported diurnal changes in O_2/Ar saturation in the Southern Ocean and coastal Antarctic waters and showed short-term variability in

NCP that questioned the applicability of the steady state assumption. These pioneering studies were conducted in marine regions that differ greatly from the oligotrophic North Pacific Subtropical Gyre (NPSG) but raised the question of whether metabolic rates in oligotrophic subtropical gyres are sufficiently large to also cause measurable diel cycles in O_2/Ar saturation.

In this paper, we demonstrate the utility of using diel changes in O_2/Ar saturation to estimate mixed layer gross O_2 production (GOP), MCR, and net oxygen production (NOP) in the oligotrophic North Pacific Ocean and compare our estimates to primary productivity values from in situ 12 h daytime ^{14}C incubations, MCR inferred from in vivo electron transport system (ETS) activity, and with previous productivity and MCR estimates at Station ALOHA (A Long-term Oligotrophic Habitat Assessment).

2. Analytical Methods

The fieldwork was conducted aboard the R/V *Kilo Moana* during a 2 week oceanographic cruise (11–25 March 2014) at Station ALOHA (22°45′N, 158°00′W), within the NPSG. This location is the site of the Hawaii Ocean Time-series (HOT) program [*Karl and Lukas*, 1996] (http://hahana.soest.hawaii.edu/hot/). Vertical profiles of temperature, salinity, dissolved O_2, and fluorescence were conducted every 4 h using a conductivity-temperature-depth (CTD) package (Sea-Bird SBE 911Plus) connected to a rosette. The O_2 and fluorescence sensors were calibrated with discrete samples following HOT procedures (http://hahana.soest.hawaii.edu/hot/methods/results.html).

Samples for O_2/Ar analyses were collected in triplicate at three different depths within the mixed layer (5, 25, and 45 m) with 12 L Niskin® bottles attached to the CTD rosette. The profiling CTD sampling was supplemented with the deployment of a single, 1.2 L Niskin® bottle at a depth of 25 m between CTD casts to provide a greater temporal resolution. Seawater samples were transferred to 12 mL Labco Exetainer® screw cap vials with rubber septa. The vials were filled using Tygon® tubing from the bottom and allowed to overflow at least 3 times their volume. Samples were poisoned with 50 μL of saturated mercuric chloride solution and, when not measured immediately, stored in the dark immersed in a 4°C water bath. Samples were measured on board within 24 h of collection.

Dissolved O_2/Ar molar ratios were measured by membrane-inlet mass spectrometry (MIMS) following *Kana et al.* [1994]. Briefly, the water sample is pumped through capillary stainless steel and Viton® tubing into a semipermeable microbore silicone membrane connected to a vacuum inlet system. After the water sample is drawn into the capillary tubing, the tubing is passed through a water bath to stabilize the sample temperature at 23°C. The gases extracted through the silicone membrane pass through a U-shaped glass tube immersed in liquid nitrogen to remove water vapor and CO_2, before entering a quadrupole mass spectrometer (Pfeiffer HiCube). For this study, masses 28, 32, and 40 were recorded. To account for drift in the signals, a standard was run every six samples (~30 min). The standard consisted of seawater collected from 25 m at Station ALOHA, 0.2 μm filtered, and equilibrated with ambient air at 23°C. Dissolved O_2 and Ar concentrations in the standard were calculated using the solubility equations reported by *García and Gordon* [1992] and *Hamme and Emerson* [2004], respectively. The precision of triplicate samples was on average 0.05% for O_2/Ar ratios.

The O_2/Ar value for the mixed layer was calculated as the mean of the values from 5, 25, and 45 m that were within the mixed layer, calculated as a density offset of 0.125 kg m^{-3} from the surface [*Suga et al.*, 2004]. On average, the standard error (SE) for the different depths represented 3% of the mean. For the single Niskin bottle deployments, the value at 25 m was assumed to be representative of the mixed layer.

MCR rates were inferred from the in vivo reduction of the tetrazolium salt 2-(*p*-iodophenyl)-3-(*p*-nitrophenyl)-5-phenyltetrazolium chloride (INT) to INT-formazan (INT-F) by ETS dehydrogenase enzymes [*Martínez-García et al.*, 2009]. A total of 14 INT reduction incubation experiments were conducted throughout the cruise. Briefly, two formaldehyde-killed controls (2% vol/vol final concentration) and three seawater samples were collected in 250 mL High Density Polyethylene bottles, spiked with a sterile 8 mM INT solution and incubated at in situ temperature for 1.5 h in the dark in on-deck incubators. After incubation, live samples were fixed by adding formaldehyde (2% vol/vol final concentration) and filtered through 0.2 μm pore size polycarbonate filters. The reduced INT-F was extracted from the filters in 1 mL 1-propanol (>99.5%) and analyzed by absorption spectrophotometry at 485 nm (Ultra Violet-2401 PC Shimadzu spectrophotometer).

The INT-F concentration was calculated using a 12-point calibration curve of pure INT-F (Sigma) dissolved in propanol. INT reduction was transformed into O_2 consumption using a MCR/INT reduction ratio of 12.8 mol O_2/mol INT-F [*Martínez-García et al.,* 2009]. We refer to MCR estimated using this method as ETS-CR. Previous vertical profiles of ETS-CR at Station ALOHA [*Martínez-García and Karl*, 2015] have shown that the ETS-CR value at 25 m is representative of the mixed layer, and therefore, integrated ETS-CR was calculated assuming a constant rate in the mixed layer.

On 13 March 2014, a 12 h in situ array was deployed to measure primary production at different depths (5, 25, 45, 75, 100, 125, and 150 m) using the ^{14}C incubation method [*Steemann Nielsen*, 1952], following HOT procedures [*Letelier et al.,* 1996] (http://hahana.soest.hawaii.edu/hot/methods/pprod.html). We refer to ^{14}C-based primary productivity as ^{14}C-PP. Depth-integrated ^{14}C-PP to 200 m was obtained by applying the trapezoidal rule, assuming zero light assimilation at a depth of 200 m [*Letelier et al.,* 1996].

3. Determination of NOP, MCR, and GOP

3.1. Gas Transfer Velocity

The gas transfer velocity for O_2, k_{O2}, was calculated using the quadratic dependence reported by *Wanninkhof* [2014]:

$$k_{O2} = 0.251(U_{10})^2\left(\frac{Sc\ (O_2)}{660}\right)^{\frac{1}{2}} \quad (1)$$

where $Sc(O_2)$ is the Schmidt number for O_2, calculated using the updated temperature-dependent equations reported by *Wanninkhof* [2014] for seawater. Gas transfer velocities were calculated from sea surface temperature and wind speed, normalized to a height of 10 m above sea surface [*Smith*, 1988], measured at 3.4 m at the Woods Hole Oceanographic Institution-Hawaii Ocean Time Series Station (WHOTS) mooring (22°45′N, 157°55′W) and available online at http://uop.whoi.edu/projects/WHOTS/whotsdata.htm.

For NOP calculations using the steady state assumption (see section 3.2), we used a 20 day weighting technique to determine the weighted gas transfer velocity, k_w, in order to account for changes in wind speed prior to the measurements [*Reuer et al.,* 2007]. The mixed layer depth (MLD) prior to the cruise was determined using a linear regression between daily mean MLD and the average wind speed of the previous 5 days ($r = 0.957$; $p < 0.0001$; see Figure S1 in the supporting information).

3.2. *Prior*-NOP

The traditional way of determining NOP in the mixed layer from O_2/Ar measurements assumes that the O_2/Ar saturation is in steady state and that vertical and lateral mixing are negligible [*Cassar et al.,* 2011; *Hamme et al.,* 2012]. Under these conditions, NOP (mmol O_2 m^{-2} d^{-1}) is balanced by the air-water flux of biological O_2 and can be estimated from individual O_2/Ar measurements as follows:

$$\mathrm{NOP} = k_w\Delta(O_2/\mathrm{Ar})[O_2]_{\mathrm{sat}}\rho \quad (2)$$

where k_w is the weighted gas transfer velocity for O_2 (m d^{-1}, see section 3.1), $[O_2]_{sat}$ is the O_2 saturation at equilibrium with the atmosphere (mmol kg^{-1}), ρ is the density of seawater (kg m^{-3}) in the mixed layer, and $\Delta(O_2/Ar)$ is the deviation of O_2/Ar from equilibrium, determined as

$$\Delta(O_2/\mathrm{Ar}) = \left[\frac{(O_2/\mathrm{Ar})_{\mathrm{sample}}}{(O_2/\mathrm{Ar})_{\mathrm{sat}}} - 1\right] \quad (3)$$

where $(O_2/Ar)_{sample}$ is the measured ratio, and $(O_2/Ar)_{sat}$ is the ratio expected at saturation equilibrium calculated using the solubility equations of *García and Gordon* [1992] for O_2 and *Hamme and Emerson* [2004] for Ar.

Hamme et al. [2012] referred to NOP calculated using equation (2) as *prior*-NOP, as it averages over the residence time of O_2 in the mixed layer prior to the measurement, which in our cruise averaged 13 days, and assumes that NOP has been constant during that time. Because we observed diel changes in $\Delta(O_2/Ar)$ of up to 0.4%, *prior*-NOP was calculated using the daily average of $\Delta(O_2/Ar)$ values. Therefore, *prior*-NOP reported here differs from previously reported NOP values using the steady state assumption in that we used the daily average of $\Delta(O_2/Ar)$ instead of instantaneous values.

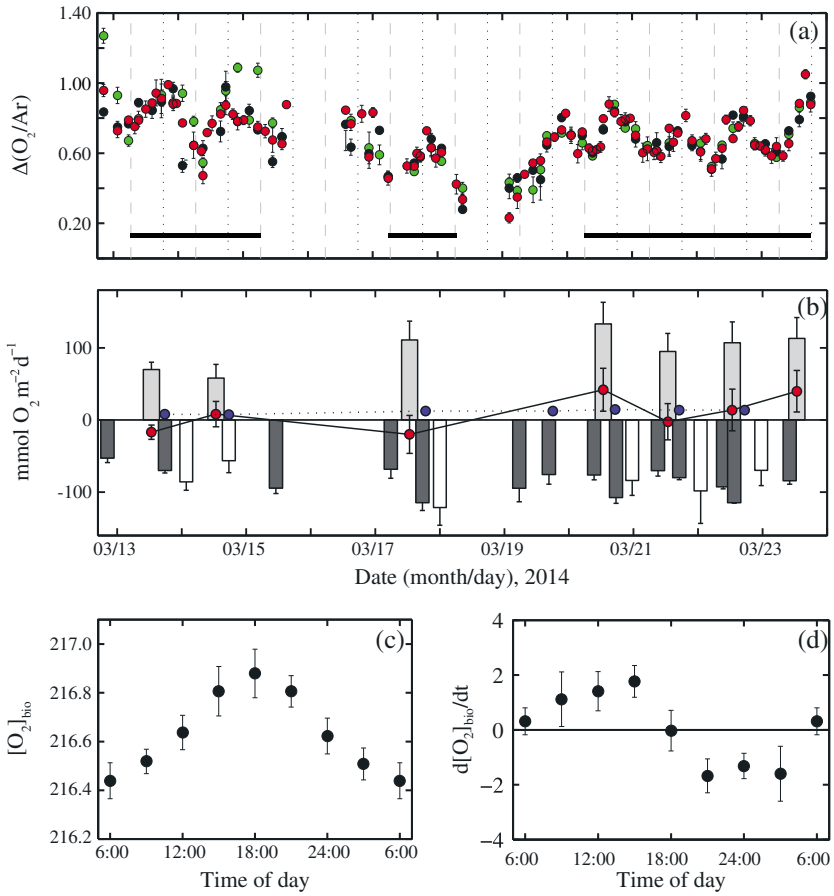


Figure 1. (a) $\Delta(O_2/Ar)$ (%) at 5 m (black), 25 m (red), and 45 m (green) at Station ALOHA in March 2014. Error bars represent the SE of triplicate samples. The dashed and dotted vertical lines represent the time of sunrise and sunset, respectively. Black horizontal bars show the periods of time when *diel* rates were calculated. (b) Integrated metabolic O_2 rates: light gray, white, and dark gray bars represent *diel*-GOP, *diel*-CR, and ETS-CR, respectively; red and blue circles represent *diel*-GOP and *prior*-NOP, respectively. Error bars for ETS-CR and *prior*-NOP represent the SE, and for *diel*-GOP, *diel*-CR, and *diel*-NOP error bars represent the estimated uncertainty as described in section 3.4; (c) mean diel cycle of biological O_2 in $\mu mol\ L^{-1}$ throughout the day; (d) mean diel cycle of the rate of change of biological O_2 with time in $mmol\ m^{-3}\ d^{-1}$ throughout the day. Error bars in Figures 1c and 1d represent the SE of 3 h binned values.

3.3. *Diel*-NOP, *Diel*-GOP, and *Diel*-CR

The observation that $\Delta(O_2/Ar)$ in the mixed layer systematically varies throughout the day [*Hamme et al.,* 2012; *Tortell et al.,* 2014] provides another way of estimating not only NOP but also GOP and MCR from in situ measurements. $\Delta(O_2/Ar)$ decreased during the night and increased during the day (Figures 1a and 1c) due to a combination of gas exchange and biological processes [*Hamme et al.,* 2012]. From the daytime and nighttime changes in $\Delta(O_2/Ar)$, we calculated the net O_2 production during daytime, NOP_{day}, and the nighttime MCR ($mmol\ O_2\ m^{-2}\ d^{-1}$) as

$$NOP_{day} \text{ or } MCR = MLD\frac{d(\Delta(O_2/Ar))}{dt}[O_2]_{sat}\rho + \overline{k_{O2}\Delta(O_2/Ar)[O_2]_{sat}\rho} \quad (4)$$

where MLD is the mean mixed layer depth (m) during the time period considered. The rate of change of $\Delta(O_2/Ar)$ during the night and day was estimated using a linear regression of $\Delta(O_2/Ar)$ with time. The second term on the right side of equation (4) is the mean air-gas exchange of biological O_2 during the time period considered, with k_{O2} being the (nonweighted) gas transfer velocity for O_2 (see section 3.1). Assuming that MCR is the same during the night and day, GOP ($mmol\ m^{-2}\ d^{-1}$) was calculated as

$$GOP = \frac{t_D}{24}NOP_{day} - \frac{t_D}{24}MCR \quad (5)$$

Table 1. *Prior* and *Diel* Rates at Station ALOHA

			Prior-NCP			
Day[a]	MLD[b] (m)	*kw*[c] (m d^{-1})	$\Delta(O_2/Ar)$[b] (%)	$[O_2]_{eq}$[b] (μmol L^{-1})	*Prior*-NCP[d] (mmol m^{-2} d^{-1})	*Prior*-NCP[e] (mmol m^{-2} d^{-1})
13–14	60 ± 5	4.4	0.82 ± 0.03	214.6 ± 0.1	7.9 ± 0.3	7.9 ± 0.3
14–15	45 ± 2	5.0	0.74 ± 0.03	213. 8 ± 0.3	7.8 ± 0.4	7.8 ± 0.4
17–18	104 ± 2	6.8	0.58 ± 0.03	215.5 ± 0.2	8.5 ± 0.4	12.3 ± 0.4
19–20	100 ± 3	6.8	0.59 ± 0.04	215.4 ± 0.1	8.7 ± 0.6	12.5 ± 0.6
20–21	99 ± 1	6.9	0.71 ± 0.03	215.6 ± 0.1	10.6 ± 0.4	14.5 ± 0.4
21–22	92 ± 4	7.0	0.65 ± 0.02	215.5 ± 0.1	9.8 ± 0.3	13.6 ± 0.3
22–23	86 ± 3	7.0	0.67 ± 0.03	215.7 ± 0.1	10.1 ± 0.4	13.8 ± 0.4
			Diel Rate Estimates			
Day[a]	MLD[b] (m)	$d[O_2]_{bio}/dt$[f] (mmol m^{-3} d^{-1})	F_{GE}[g] (mmol m^{-3} d^{-1})	*Diel*-CR (mmol m^{-3} d^{-1})	*Diel*-GOP (mmol m^{-3} d^{-1})	*Diel*-NOP (mmol m^{-3} d^{-1})
13	60 ± 8	0.83	0.09		1.20 ± 0.17	−0.28 ± 0.17
13–14	53 ± 6	−1.56	0.07	−1.48 ± 0.19		
14	47 ± 2	1.19	0.19		1.20 ± 0.39	0.18 ± 0.39
14–15	40 ± 2	−0.84	0.29	−0.55 ± 0.37		
17	105 ± 2	0.87	0.07		1.06 ± 0.25	−0.19 ± 0.25
17–18	104 ± 2	−1.31	0.06	−1.25 ± 0.24		
20	103 ± 3	1.15	0.09		1.31 ± 0.30	0.42 ± 0.30
20–21	94 ± 3	1.00	0.11	−0.89 ± 0.21		
21	95 ± 6	0.97	0.08		1.00 ± 0.27	−0.03 ± 0.27
21–22	85 ± 2	−1.23	0.08	−1.16 ± 0.49		
22	90 ± 4	1.34	0.07		1.18 ± 0.34	0.16 ± 0.34
22–23	79 ± 2	−0.96	0.08	−0.88 ± 0.25		
23	83 ± 8	1.84	0.12		1.36 ± 0.35	0.48 ± 0.35
Mean ± SE				−1.04 ± 0.13	1.19 ± 0.05	0.11 ± 0.11

[a]Day in March 2014.
[b]Mean ± standard error (SE) during the 24 h (*Prior*-NCP) or 12 h (Diel Rate Estimates) periods.
[c]Weighted gas transfer velocity, calculated using *Wanninkhof* [2014] wind speed relationship.
[d]*Prior*-NCP before the entrainment correction.
[e]*Prior*-NCP corrected for entrainment.
[f]Rate of change of biological O_2 during the 12 h period considered.
[g]Air-gas exchange correction (second term in equation (4)).

where t_D is the daytime length in hours. Note that MCR has a negative value. Similarly, NOP (mmol m^{-2} d^{-1}) was calculated as

$$\mathrm{NOP} = \frac{t_D}{24}\mathrm{NOP_{day}} + \frac{t_N}{24}\mathrm{MCR} \tag{6}$$

where t_D is the night length in hours. We refer to MCR, GOP, and NOP calculated using equations (4)–(6), respectively, as *diel*-CR, *diel*-GOP, and *diel*-NOP. When possible, in equations (5) and (6) we used the mean *diel*-CR from the previous and following night with respect to NOP_{day}. *Diel*-NOP averages over a shorter period of time (24 h) than *prior*-NOP, and therefore, day-to-day variability is inherent, but it does not rely on the assumption of steady state conditions. It should be noted that small errors in NOP_{day} and MCR may cause large errors in *diel*-NOP estimated using equation (6).

3.4. Assessment of Vertical Mixing

One of the assumptions often made when quantifying NOP based on O_2/Ar measurements is that the influence of horizontal and vertical mixing is negligible. At Station ALOHA, horizontal advection and diffusion are thought to be small in terms of the O_2 balance, due to weak horizontal gradients [*Emerson et al.,* 1995]. However, it has been shown that entrainment of water from below the mixed layer can be a potentially significant source of error for triple O_2 isotope estimates of GOP [*Nicholson et al.,* 2012; *Quay et al.,* 2010].

During the sampling period, we observed a clear entrainment event on 16 March, when high wind speeds during the night of 15 March were followed by a deepening of the mixed layer (Table 1, see Figure S2 in the supporting information). The wind speed at 10 m above sea surface (u_{10}) evolved from 7.5 ± 0.8 m s^{-1}

(mean ± standard deviation (SD)) for 13–14 March to 11.9 ± 1.6 (SD) m s^{-1} during 15–17 March, when u_{10} reached values of up to 14.4 m s^{-1}. From 18 March until the end of the cruise mean u_{10} was 8.5 ± 0.9 (SD) m s^{-1}.

Although vertical O_2 profiles from CTD casts showed weak vertical gradients below the mixed layer, two O_2/Ar profiles (0–1000 m) taken prior to and after the high-wind event showed that $\Delta(O_2/Ar)$ decreased below the mixed layer. We estimated the entrainment flux, E (mmol O_2 m^{-2} d^{-1}), following *Emerson et al.* [2008]:

$$E = \frac{dh}{dt}\left([O_2]^{E}_{bio} - [O_2]^{ML}_{bio}\right) \quad (7)$$

where $\frac{dh}{dt}$ is the rate of change of depth of the mixed layer with time, the superscripts E and ML refer to entrained seawater and mixed layer seawater, respectively, and $[O_2]_{bio}$ is the biological O_2, calculated as

$$[O_2]_{bio} = \frac{(O_2/Ar)_{sample}}{(O_2/Ar)_{sat}}[O_2]_{eq} \quad (8)$$

$[O_2]^{E}_{bio}$ was determined from the profile taken before the storm by interpolating $[O_2]_{bio}$ with depth and taking the average of the entrained water. *Prior*-NOP values were corrected for entrainment by subtracting E from the right-hand term of equation (2), which equaled −3.8 mmol O_2 m^{-2} d^{-1}. This correction only affected *prior*-NOP estimates, increasing the mean value by ~30%. Any potential entrainment occurring prior to the cruise was not taken into account.

3.5. Error Analysis

The estimated errors in the rates were calculated by propagating the uncertainty of individual terms: k ± 20% [*Wanninkhof*, 2014], $[O_2]_{eq}$ ± 0.2% [*Emerson et al.,* 1995], $\Delta(O_2/Ar)$ ± standard deviation (SD) over a 24 h cycle (~ ± 12%), and $d(\Delta(O_2/Ar))/dt$ ± the standard error in the slope (~ ± 20%). This analysis resulted in an error of ± 35% for *prior*-NOP. The mean uncertainty in NOP_{day}, MCR, and GOP was ± 25%.

4. Results and Discussion

4.1. Diel $\Delta(O_2/Ar)$ Variability and Its Implications

Discrete $\Delta(O_2/Ar)$ values were supersaturated during the entire cruise indicating a net biological production of O_2 in the mixed layer for the sampling period (Figure 1a), consistent with previously reported values at Station ALOHA [*Emerson et al.,* 1997; *Hamme and Emerson*, 2006; *Juranek and Quay*, 2005; *Quay et al.,* 2010].

$\Delta(O_2/Ar)$ values increased during the day and decreased at night, with minimum and maximum values normally observed near sunrise and sunset, respectively (Figures 1a and 1c). Therefore, the net production of O_2 started right after sunrise and lasted until sunset, except for a few occasions in which the $\Delta(O_2/Ar)$ minimum was 1–3 h after sunrise. The daily maximum in $\Delta(O_2/Ar)$ occurred at or slightly after sunset. During the first 3 days of sampling the water was more stratified, and on some occasions the $\Delta(O_2/Ar)$ values at 5, 25, and 45 m differed substantially, with the value at 45 m being larger, likely due to net O_2 production without active exchange with the atmosphere [*Juranek and Quay*, 2005]. There were a few periods in our time series that we did not include in our rate calculations to avoid misinterpreting the trends. These included (i) the night on 13 March, as we only had three data points and there were physical-chemical gradients within the mixed layer, (ii) the day on 15 March, which coincided with the entrainment event, (iii) the night on 17 March, as the data were highly scattered, and (iv) on 19 March, when the $\Delta(O_2/Ar)$ values did not show the expected pattern and kept increasing during the night. This latter effect is likely due to horizontal advection and might represent a limitation of this method in areas of large spatial heterogeneity. In those cases, it is still possible to determine diel metabolic rates following a Lagrangian sampling design [e.g., *Hamme et al.,* 2012]. Figure 1a shows the 24 h cycles that were used in our calculations.

The daily pattern in $\Delta(O_2/Ar)$ is evident when the data are binned into 3 h daytime intervals and averaged into a mean diel cycle (Figure 1c). Figure 1d shows the mean daily cycle for the rate of change in biological O_2 ($d[O_2]_{bio}/dt$) also binned into 3 h intervals throughout the day. Near sunset and sunrise, the $d[O_2]_{bio}/dt$ is close to zero, as the system is switching from net autotrophic to net heterotrophic and vice

versa. Mean MCR rates were relatively constant throughout the night. During the day, photosynthesis varied as a function of sun irradiance, but the binned data at 9:00, 12:00, and 15:00 were not significantly different. Also, *diel*-GOP values calculated using the slope of $\Delta(O_2/Ar)$ with time or using the difference of $\Delta(O_2/Ar)$ between sunset and sunrise were not significantly different.

We observed diel changes in $\Delta(O_2/Ar)$ values that ranged from 0.2 to 0.4% (Figure 1a), superimposed on a mean $\Delta(O_2/Ar)$ value of 0.70 ± 0.14% (SD). By comparison, *Hamme et al.* [2012] observed diel changes in $\Delta(O_2/Ar)$ of up to 0.6% in the Southern Ocean. During the present study at Station ALOHA, $\Delta(O_2/Ar)$ diel changes caused up to 21% variability (SD/mean × 100%) in *prior*-NOP rates calculated from individual measurements over 24 h periods. In oceanic regions characterized by larger GOP and MCR the variability introduced by diel changes in $\Delta(O_2/Ar)$ is expected to be larger [e.g., *Tortell et al.,* 2014], and therefore, one important implication of the observed diel $\Delta(O_2/Ar)$ pattern is that it might introduce a significant error when estimating *prior*-NOP from individual samples, especially if the samples are collected close to sunrise or sunset.

4.2. Primary and Gross O_2 Production

Volumetric *diel*-GOP ranged from 1.00 to 1.36 mmol O_2 m^{-3} d^{-1} (Table 1), and from 59 to 131 mmol O_2 m^{-2} d^{-1} (mean ± standard error, SE: 96 ± 10 mmol O_2 m^{-2} d^{-1}) when integrated over the mixed layer (Figure 1b). Part of the variability observed in depth-integrated values was driven by the deepening of the mixed layer from 54 ± 4 (SE) m prior to the high wind speed event, to 94 ± 2 (SE) m afterward. Consequently, *diel*-GOP increased from 65 ± 7 (SE) mmol O_2 m^{-2} d^{-1} to 109 ± 6 (SE) mmol O_2 m^{-2} d^{-1}. This demonstrates that when the mixed layer is shallow at Station ALOHA, rates of GOP within the mixed layer might account for only ~60% of GOP integrated for the photic zone [*Quay et al.,* 2010]. This is important because based on HOT climatological data, approximately 50% of the time the MLD is shallower than 55 m at Station ALOHA. Accordingly, the integrated ^{14}C-PP from in situ 12 h daytime ^{14}C incubations conducted on 13 March was 48 ± 1.1 mmol C m^{-2} d^{-1}, and the integrated ^{14}C-PP for the top 55 m accounted for only 50% of the total.

The mean mixed layer *diel*-GOP observed after the mixing event, 109 ± 6 (SE) mmol O_2 m^{-2} d^{-1}, that integrated over approximately the upper 100 m of the water column, is in the upper range of previously reported GOP derived from ^{18}O incubations (^{18}O-GOP), and within the range of GOP derived from in situ measurements of triple isotopic composition of dissolved O_2 ($^{17}\Delta$-GOP) [*Juranek and Quay*, 2005; *Quay et al.,* 2010]. *Diel*-GOP and $^{17}\Delta$-GOP are expected to be larger than ^{18}O-GOP, as they are not affected by containment effects [*Juranek and Quay*, 2005; *Quay et al.,* 2010]. On the other hand, both $^{17}\Delta$-GOP and ^{18}O-GOP represent measures of total O_2 production via the splitting of water, and therefore, overestimate gross production by the extent that O_2 is consumed by the Mehler reaction and photorespiration [*Bender et al.,* 1999; *Juranek and Quay*, 2012].

Despite being the most widely used method to measure productivity, it is unclear whether the ^{14}C method measures GPP, net primary production, or a value in between [*Bender et al.,* 1999; *Marra*, 2002]. The ratio of ^{18}O-GOP/^{14}C-PP (12 h) in the photic layer at Station ALOHA has been reported to range from 1.8 ± 0.4 in winter to 2.0 ± 0.5 in summer, whereas $^{17}\Delta$-GOP/^{14}C-PP (12 h) ratios ranged from 2.2 in the winter to 2.8 in the summer [*Quay et al.,* 2010]. The ratio of GOP derived from fast repetition rate fluorometry to ^{14}C-PP (12 h) at the surface varied from 1.9 in winter to 2.3 in fall, for light-normalized data at Station ALOHA [*Corno et al.,* 2006]. During this study we obtained a *diel*-GOP/^{14}C-PP (12 h) for the mixed layer of 2.7 ± 0.1 mol O_2/mol C, which is in the upper range of previously reported data at Station ALOHA, and more in line with $^{17}\Delta$-GOP/^{14}C-PP ratios. It must be taken into account that the ratio was calculated using a single ^{14}C-PP profile that occurred before the mixing event, and most of our *diel*-GOP values were estimated afterward. Also, mixed layer *diel*-GOP/^{14}C-PP is expected to change with mixed layer depth, as the GOP/^{14}C-PP ratio decreases with depth at Station ALOHA [*Corno et al.,* 2006*; Quay et al.,* 2010] to a value approaching 1.0 at 100 m [*Quay et al.,* 2010].

With respect to *prior*-NOP values, which have less variability than *diel*-NOP, the ratio of NOP/GOP (mol O_2/mol O_2) in the mixed layer averaged 0.12 ± 0.01. The ratio of mean *diel*-NOP and mean GOP yielded 0.09. In comparison with previous work at Station ALOHA, *Quay et al.* [2010] reported mixed layer *prior*-NOP/$^{17}\Delta$-GOP ratios of 0.22 ± 0.08 and 0.12 ± 0.05 during summer and winter, respectively, with the annual mean being 0.19 ± 0.08 in the mixed layer.

4.3. Microbial Community Respiration

There was excellent agreement between *diel*-CR and ETS-CR. *Diel*-CR ranged from −0.55 to −1.48 (mean ± SE: −1.04 ± 0.13) mmol O_2 m^{-3} d^{-1} (Table 1), whereas ETS-CR ranged from −0.67 to −1.38 (−0.97 ± 0.03) mmol O_2 m^{-3} d^{-1} (see Table S1 in the supporting information). The smallest *diel*-CR rate corresponded to the start of the high-wind event (see section 3.1 and Table 1) and could be partly due to an overestimation of k_{O2} at high wind speeds. Integrated *diel*-CR and ETS-CR were also in good agreement (Figure 1b), with mean values of −86 ± 14 (SE) and −85 ± 5 (SE) mmol O_2 m^{-2} d^{-1}, respectively.

Both *diel*-CR and ETS-CR volumetric rates were within the ranges of −0.55 to −1.48 and of −0.31 to −1.54 mmol O_2 m^{-3} d^{-1} reported in the mixed layer at Station ALOHA by *Williams et al.* [2004] using the Winkler method, and by *Martínez-García and Karl* [2015] using the ETS method, respectively. The excellent agreement between in situ *diel*-CR and in vitro methods (ETS and Winkler) might indicate that the mismatch between in situ and in vitro NCP estimates [*Williams et al.,* 2013] is due to an underestimation of primary production from in vitro methods [e.g., *Juranek and Quay*, 2005; *Quay et al.,* 2010; *Westberry et al.,* 2012].

During the sampling period, we observed larger variability in *diel*-CR and ETS-CR (32% and 23%, respectively) than in *diel*-GOP (11%), and the switch between positive and negative *diel*-NCP seemed to be mainly driven by changes in *diel*-CR rather than *diel*-GOP (Figure 1b). This is consistent with observations by *Mouriño-Carbadillo* [2009] showing that MCR is at least as important as primary production in controlling the metabolic status of the upper ocean.

4.4. Net Oxygen and Carbon Production in the Mixed Layer

Mixed layer *prior*-NOP ranged from 7.7 to 14.4 mmol O_2 m^{-2} d^{-1} (mean ± SE: 11.8 ± 1.1 mmol O_2 m^{-2} d^{-1}), whereas *diel*-NOP ranged from a net O_2 consumption of 20 mmol O_2 m^{-2} d^{-1} to a net O_2 production of 42 mmol O_2 m^{-2} d^{-1} but averaged +9.2 ± 9.3 (SE) mmol O_2 m^{-2} d^{-1} (Figure 1b). The large variability observed in *diel*-NOP indicates that the metabolic status of the mixed layer may be more variable over shorter time scales than previously thought based on in situ geochemical tracers and ^{14}C primary productivity [*Hamme et al.,* 2012; *Tortell et al.,* 2014]. Daily individual estimates of *diel*-NOP from this study expand the range of *prior*-NOP previously measured at Station ALOHA from O_2/Ar and O_2/N_2 measurements, which range from 13 to 19 mmol O_2 m^{-2} d^{-1} [*Emerson et al.,* 1997, 2008; *Hamme and Emerson*, 2006; *Juranek and Quay*, 2005; *Quay et al.,* 2010]. This most likely relates to the fact that *diel*- and *prior*-NOP represent different time scales. It is quite remarkable and perhaps coincidental that despite the different integration times, mean *prior*- and *diel*-NOP values were in relatively good agreement when averaged over the entire sampling period (>10 days). The rate of change in the daily mean $\Delta(O_2/Ar)$ values with time after the mixing event provides another way of estimating NOP [*Hamme et al.,* 2012], yielding 13.2 ± 4.6 mmol O_2 m^{-2} d^{-1}, which is also in excellent agreement with the mean *prior*-NOP for that time period (13.3 ± 0.4 mmol O_2 m^{-2} d^{-1}).

Quantification of GOP and MCR is critical to understand the net metabolic status of the upper ocean when using an O_2 mass balance. To further extrapolate NCP based on O_2/Ar into C units, it is necessary to know both the photosynthetic ($PQ = \Delta O_2:\Delta CO_2$) and respiratory ($RQ = \Delta CO_2:\Delta O_2$) quotients. Depending on the nitrogen substrate used to support primary production, the PQ can range from 1.1 for ammonia (regenerated production) to 1.4 for nitrate (new production) [*Laws*, 1991]. In the NPSG approximately 90% of primary production is regenerated [*Karl*, 1999], and hence, the PQ is expected to be much closer to 1.1 than 1.4. In addition, up to 50% of the new production is supported by N_2 fixation instead of nitrate [*Karl et al.,* 1997]. On the other hand, the RQs for bacterial growth on most organic compounds range between 0.67 and 1.24 [*Williams and del Giorgio*, 2005], and for algal cell and planktonic material is 0.89 [*Hedges et al.,* 2002; *Williams and Robertson*, 1991]. The calculation of NCP from GOP and MCR is highly sensitive to the quotients used to convert O_2 to C. In addition, the direct conversion of NOP to NCP can be problematic if the O_2 to C stoichiometry differs from respiration and photosynthesis or if mixotrophic or chemolithoautotrophic growth is common [*Karl*, 2014].

Applying a PQ of 1.1 and a RQ of 0.89, we obtain a mean GPP of 85 ± 10 (SE) mmol C m^{-2} d^{-1} and a mean MCR of −77 ± 13 (SE) mmol C m^{-2} d^{-1}. This yields a mean NCP of 9 ± 10 (SE) mmol C m^{-2} d^{-1} for the mixed layer,

indicating that the mixed layer was net autotrophic during the sampling period. However, extrapolating these results to the entire euphotic zone might yield a different metabolic balance as ^{18}O-GOP and ^{14}C-PP decrease more rapidly with depth than MCR [*Letelier et al.,* 1996; *Martínez-García and Karl*, 2015; *Quay et al.,* 2010].

5. Conclusions and Implications

This study demonstrates the utility of using diel changes in $\Delta(O_2/Ar)$ within the mixed layer to estimate in situ GOP, MCR, and NOP in the oligotrophic ocean, from which we can infer the metabolic status of the mixed layer. MCR estimates from $\Delta(O_2/Ar)$ changes were in very good agreement with ETS-CR and previously reported MCR values at Station ALOHA. Despite the large fluctuations observed in *diel*-NOP, when averaged over the sampling period *diel*- and *prior*-NOP were in relatively good agreement. A large part of the variability observed in *diel*-NOP was driven by changes in MCR. Our estimates showed that, applying a PQ of 1.1 and a RQ of 0.89, the mixed layer was net autotrophic during the sampling period, with a mean NCP of 9 ± 10 mmol C m^{-2} d^{-1}.

Diel-GOP, *diel*-CR, and *diel*-NOP estimates might be used to identify rapid community responses to environmental forcing and help understand the mechanisms controlling the biological pump.

Acknowledgments

We thank the captain and crew of the R/V *Kilo Moana* for their assistance in field operations, T. Clemente and K. Björkman for ^{14}C measurements, L. A. Fujieki for data processing, D. A. del Valle for help with the MIMS, and B. Barone for helpful discussion. Thoughtful comments from Peter J. le B. Williams and Maria Prokopenko significantly improved the manuscript. This research was supported by the National Science Foundation (NSF) through the Center for Microbial Oceanography: Research and Education (C-MORE; EF04-24599) and the Gordon and Betty Moore Foundation. This publication used data from the WHOTS mooring, which is supported by the National Oceanic and Atmospheric Administration (NOAA) through the Cooperative Institute for Climate and Ocean Research (CICOR) under grants NA17RJ1223 and NA090AR4320129 and by NSF grants OCE-0327513, OCE-752606, and OCE-0926766. S.M-G. was funded by a Fulbright-MEC. S.F. and S.M-G. were funded by C-MORE fellowships. Data are freely available at http://hahana.soest.hawaii.edu/cmoreDS/interface.html and upon request.

The Editor thanks Peter Williams and Maria Prokopenko for their assistance in evaluating this paper.

References

Bender, M., J. Orchardo, M. L. Dickson, R. Barber, and S. Lindley (1999), In vitro O_2 fluxes compared with ^{14}C production and other rate terms during the JGOFS Equatorial Pacific experiment, *Deep Sea Res., Part I*, *46*, 637–654, doi:10.1016/S0967-0637(98)00080-6.

Cassar, N., P. J. DiFiore, B. A. Barnett, M. L. Bender, A. R. Bowie, B. Tilbrook, K. Petrou, K. J. Westwood, S. W. Wright, and D. Lefevre (2011), The influence of iron and light on net community production in the Subantarctic and Polar Frontal Zones, *Biogeosciences*, *8*, 227–237, doi:10.5194/bg-8-227-2011.

Corno, G., R. M. Letelier, M. R. Abbott, and D. M. Karl (2006), Assessing primary production variability in the North Pacific subtropical gyre: A comparison of fast repetition rate fluorometry and ^{14}C measurements, *J. Phycol.*, *421*, 51–60.

del Giorgio, P. A., J. J. Cole, and A. Cimbleris (1997), Respiration rates in bacteria exceed phytoplankton production in unproductive aquatic systems, *Nature*, *385*, 148–151, doi:10.1038/385148a0.

Duarte, C. M., A. Regaudie-de-Gioux, J. M. Arrieta, A. Delgado-Huertas, and S. Agustí (2013), The oligotrophic ocean is heterotrophic, *Annu. Rev. Mar. Sci.*, *5*, 551–569, doi:10.1146/annurev-marine-121211-172337.

Ducklow, H. W., and S. C. Doney (2013), What is the metabolic state of the oligotrophic ocean? A debate, *Annu. Rev. Mar. Sci.*, *5*, 525–533, doi:10.1146/annurev-marine-121211-172331.

Emerson, S., P. D. Quay, C. Stump, D. Wilbur, and R. Schudlich (1995), Chemical tracers of productivity and respiration in the subtropical Pacific Ocean, *J. Geophys. Res.*, *100*, 15,873–15,887, doi:10.1029/95JC01333.

Emerson, S., P. Quay, D. Karl, C. Winn, L. Tupas, and M. Landry (1997), Experimental determination of the organic carbon flux from open-ocean surface waters, *Nature*, *389*, 951–954, doi:10.1038/40111.

Emerson, S., C. Stump, and D. Nicholson (2008), Net biological oxygen production in the ocean: Remote in situ measurements of O_2 and N_2 in surface waters, *Global Biogeochem. Cycles*, *22*, GB3023, doi:10.1029/2007GB003095.

García, H. E., and L. I. Gordon (1992), Oxygen solubility in seawater: Better fitting equations, *Limnol. Oceanogr.*, *37*, 1307–1312, doi:10.4319/lo.1992.37.6.1307.

Hamme, R. C., and S. R. Emerson (2004), The solubility of neon, nitrogen and argon in distilled water and seawater, *Deep Sea Res., Part I*, *51*, 1517–1528.

Hamme, R. C., and S. R. Emerson (2006), Constraining bubble dynamics and mixing with dissolved gases: Implications for productivity measurements by oxygen mass balance, *J. Mar. Res.*, *64*, 73–95, doi:10.1357/002224006776412322.

Hamme, R. C., et al. (2012), Dissolved O_2/Ar and other methods reveal rapid changes in productivity during a Lagrangian experiment in the Southern Ocean, *J. Geophys. Res.*, *117*, C00F12, doi:10.1029/2011JC007046.

Hedges, J. I., J. A. Baldock, Y. Gélinas, C. Lee, M. L. Peterson, and S. G. Wakeham (2002), The biochemical and elemental composition of marine plankton: A NMR perspective, *Mar. Chem.*, *78*, 47–63, doi:10.1016/S0304-4203(02)00009-9.

Juranek, L. W., and P. D. Quay (2005), In vitro and in situ gross primary and net community production in the North Pacific Subtropical Gyre using labeled and natural abundance isotopes of dissolved O_2, *Global Biogeochem. Cycles*, *19*, GB3009, doi:10.1029/2004GB002384.

Juranek, L. W., and P. D. Quay (2012), Using triple isotopes of dissolved oxygen to evaluate global marine productivity, *Annu. Rev. Mar. Sci.*, *5*, 503–524, doi:10.1146/annurev-marine-121211-172430.

Kaiser, J., M. K. Reuer, B. Barnett, and M. L. Bender (2005), Marine productivity estimates from continuous O_2/Ar ratio measurements by membrane inlet mass spectrometry, *Geophys. Res. Lett.*, *32*, L19605, doi:10.1029/2005GL023459.

Kana, T. M., C. Darkangelo, M. D. Hunt, J. B. Oldham, G. E. Bennett, and J. C. Cornwell (1994), Membrane inlet mass spectrometer for rapid high-precision determination of N_2, O_2, and Ar in environmental water samples, *Anal. Chem.*, *66*, 4166–4170, doi:10.1021/ac00095a009.

Karl, D. M. (1999), A sea of change: Biogeochemical variability in the North Pacific Subtropical Gyre, *Ecosystems*, *2*, 181–214, doi:10.1007/s100219900068.

Karl, D. M. (2014), Solar energy capture and transformation in the sea, *Elem. Sci. Anthropocene*, *2*, 000021, doi:10.12952/journal.elementa.000021.

Karl, D. M., and M. J. Church (2014), Microbial oceanography and the Hawaii Ocean Time-series programme, *Nat. Rev. Microbiol.*, *12*, 699–713, doi:10.1038/nrmicro3333.

Karl, D. M., and R. Lukas (1996), The Hawaii Ocean Time-series (HOT) program: Background, rationale and field implementation, *Deep Sea Res., Part II*, *43*, 129–156, doi:10.1016/0967-0645(96)00005-7.

Karl, D. M., R. M. Letelier, L. M. Tupas, J. E. Dore, J. R. Christian, and D. V. Hebel (1997), The role of nitrogen fixation in biogeochemical cycling in the subtropical North Pacific Ocean, *Nature*, *388*, 533–538.

Karl, D. M., E. A. Laws, P. Morris, P. J. l. Williams, and S. Emerson (2003), Metabolic balance of the open sea, *Nature*, *426*, 32, doi:10.1038/426032a.

Laws, E. A. (1991), Photosynthetic quotients, new production and net community production in the open ocean, *Deep Sea Res.*, *38*, 143–167, doi:10.1016/0198-0149(91)90059-O.

Letelier, R. M., J. E. Dore, C. D. Winn, and D. M. Karl (1996), Seasonal and interannual variations in photosynthetic carbon assimilation at Station ALOHA, *Deep Sea Res., Part II*, *43*, 467–490, doi:10.1016/0967-0645(96)00006-9.

Marra, J. (2002), Approaches to the measurement of plankton production, in *Phytoplankton Productivity and Carbon Assimilation in Marine and Freshwater Ecosystems*, edited by P. J. l. Williams, D. T. Thomas, and C. S. Reynolds, pp. 222–264, Blackwell, London.

Martínez-García, S., and D. M. Karl (2015), Microbial respiration in the euphotic zone at Station ALOHA, *Limnol. Oceanogr.*, doi:10.1002/lno.10072, in press.

Martínez-García, S., E. Fernández, M. Aranguren-Gassis, and E. Teira (2009), In vivo electron transport system activity: A method to estimate respiration in natural marine microbial planktonic communities, *Limnol. Oceanogr. Methods*, *7*, 459–469, doi:10.4319/lom.2009.7.459.

Mouriño-Carbadillo, B. (2009), Eddy-driven pulses of respiration in the Sargasso Sea, *Deep Sea Res., Part I*, *56*, 1242–1250, doi:10.1016/j.dsr.2009.03.001.

Nicholson, D. P., R. H. R. Stanley, E. Barkan, D. M. Karl, B. Luz, P. D. Quay, and S. C. Doney (2012), Evaluating triple oxygen isotope estimates of gross primary production at the Hawaii Ocean Time-series and Bermuda Atlantic Time-series Study sites, *J. Geophys. Res.*, *117*, C05012, doi:10.1029/2010JC006856.

Quay, P. D., C. Peacock, K. Björkman, and D. M. Karl (2010), Measuring primary production rates in the ocean: Enigmatic results between incubation and non-incubation methods at Station ALOHA, *Global Biogeochem. Cycles*, *24*, GB3014, doi:10.1029/2009GB003665.

Reuer, M. K., B. A. Barnett, M. L. Bender, P. G. Falkowski, and M. B. Hendricks (2007), New estimates of Southern Ocean biological production rates from O_2/Ar ratios and the triple isotope composition of O_2, *Deep Sea Res., Part I*, *54*, 951–974, doi:10.1016/j.dsr.2007.1002.1007.

Smith, S. D. (1988), Coefficients for sea surface wind stress, heat flux, and wind profiles as a function of wind speed and temperature, *J. Geophys. Res.*, *93*, 15,467–15,472, doi:10.1029/JC093iC12p15467.

Steemann Nielsen, E. (1952), The use of radioactive carbon (C^{14}) for measuring organic production in the sea, *J. Cons. Int. Explor. Mer.*, *18*, 117–140.

Suga, T., K. Motoki, Y. Aoki, and A. M. Macdonald (2004), The North Pacific climatology of winter mixed layer and mode waters, *J. Phys. Oceanogr.*, *34*, 3–22, doi:10.1175/1520-0485(2004)034<0003:TNPCOW>2.0.CO;2.

Tortell, P. D., E. C. Asher, H. W. Ducklow, J. A. L. Goldman, J. W. H. Dacey, J. J. Grzymski, J. N. Young, S. A. Kranz, K. S. Bernard, and F. M. M. Morel (2014), Metabolic balance of coastal Antarctic waters revealed by autonomous pCO_2 and ΔO_2/Ar measurements, *Geophys. Res. Lett.*, *41*, 6803–6810, doi:10.1002/2014GL061266.

Wanninkhof, R. (2014), Relationship between wind speed and gas exchange over the ocean revisited, *Limnol. Oceanogr. Methods*, *12*, 351–362, doi:10.4319/lom.2014.4312.4351.

Westberry, T. K., P. J. l. Williams, and M. J. Behrenfeld (2012), Global net community production and the putative net heterotrophy of the oligotrophic oceans, *Global Biogeochem. Cycles*, *26*, GB4019, doi:10.1029/2011GB004094.

Williams, P. J. l. (1998), The balance of plankton respiration and photosynthesis in the open ocean, *Nature*, *394*, 55–57, doi:10.1038/27878.

Williams, P. J. l., and P. A. del Giorgio (2005), Respiration in aquatic ecosystems: History and background, in *Respiration in Aquatic Ecosystems*, edited by P. A. del Giorgio, and J. l. Williams, pp. 1–17, Oxford Univ. Press, Oxford, U. K., doi:10.1093/acprof:oso/9780198527084.003.0001.

Williams, P. J. l., and J. E. Robertson (1991), Overall plankton oxygen and carbon dioxide metabolism: The problem of reconciling observations and calculations of photosynthetic quotients, *J. Plankton Res.*, *13*, 153–169.

Williams, P. J. l., P. J. Morris, and D. M. Karl (2004), Net community production and metabolic balance at the oligotrophic ocean site, station ALOHA, *Deep Sea Res., Part I*, *51*, 1563–1578, doi:10.1016/j.dsr.2004.07.001.

Williams, P. J. l., P. D. Quay, T. K. Westberry, and M. J. Behrenfeld (2013), The oligotrophic ocean is autotrophic, *Annu. Rev. Mar. Sci.*, *5*, 535–549, doi:10.1146/annurev-marine-121211-172335.